

Low-temperature strength of Arctic structures: finite-element analysis based on integral failure criteria

Gennady B. Kryzhevich
Krylov State Research Centre, St. Petersburg, Russia

ABSTRACT

The purpose of this work is to develop reliable criteria of brittle and ductile failure that would meet the needs of finite-element analysis for welded structures in order to determine their static strength taking into account their achievable crack resistance, as well as plasticity of welded joint materials. This paper studies welded structures of marine technology operating at common and low (-40°C and lower) temperatures. New international standards for strength and reliability of Arctic oil & gas facilities, e.g. ISO 19906, require, for justifications of necessary strength margins, ultimate strength calculations taking into account possible deterioration in plasticity and crack resistance of materials and welded joints due to low temperatures. To meet these requirements, fundamental methodical issues of structural failure analysis have been solved for stress concentration areas in the limit equilibrium state. The study takes into account deterioration in plasticity of structural joints due to three-dimensional nature of their stressed state. Therefore, the analysis is performed by means of the finite-element method and corresponding integral criteria for initiation of fracture-like defects, formulated taking into account the state of the art in failure mechanics.

Comparison of analytical and experimental data has shown that the integral ductile failure criterion suggested in this paper as a substitute for conventional local criteria makes ultimate strength calculations considerably more accurate. These integral criteria lie in the basis of the new variant of the finite-element approach to calculations of ultimate low-temperature strength and operational safety of Arctic structures.

KEYWORDS: Arctic structures; Failure mechanics, Ultimate strength; Failure criteria; Low-temperature strength.

1. INTRODUCTION

Current certification requirements for structures of Arctic ships and oil & gas platforms are given in the Rules of leading classification societies and ISO 19906 standard. Basically, these requirements describe how to assign and check performance parameters of materials and welded joints at low temperatures. The requirements to the parameters take into account a very important peculiarity of steels, i.e. considerable deterioration in their mechanical properties due to low temperature (so-called ductile-brittle transition), which results in

considerably lower crack resistance of steels and makes brittle structural failures more likely to occur. Main contributors to brittle failure are low temperature and high stiffness of stress-strain state due to stress concentrators, as well as due to manufacturing and operational defects of structures. Along with it, design experience of Arctic ships and offshore platforms (Wallin K., Karjalainen-Roikonen P. 2016; Horn A.M., Hauge M., 2011; Hauge M., 2012) shows that current crack resistance requirements to welded joints of thick-plated structures are impracticable to meet in some cases because they would make construction costs too high. From the formal standpoint, failure to meet the requirements would result in either prohibition of low-temperature operation for these Arctic structures or the necessity to construct them using very expensive materials (both main and auxiliary) and technologies. However, in certain cases, thin-plated structures with low stress concentrations at their joints may show sufficient actual strength margins at low temperatures, even though their materials have rather low crack resistance and their construction technologies are relatively simple. To estimate these strength margins, it is extremely necessary to develop and justify new calculation methods for low-temperature strength.

Another possible approach to ensuring low-temperature strength is totally different. To increase cost efficiency of Arctic structures and make the results of their strength calculations more reliable, it is possible, instead of stating tough requirements to crack resistance of their materials and welded joints, to perform direct stress-strength calculation for their most stressed zones where brittle or ductile failures are the most likely to occur. Sadly, as of now, there are no specific recommendations on how to perform such calculations. Therefore, to calculate limit state in presence of low temperatures and stress concentrators, it is also necessary to develop corresponding failure criteria that would be based on the finite-element method. Kryzhevich G.B. (2017) suggests main approaches to this task based on numerical calculations of welded structures and demonstrates that calculation results will be much more accurate if failure criteria are developed taking into account the spatial nature of stress-strain state at stress concentration zones. Conventional approaches to setting failure criteria in terms of acceptable stresses and limit plastic strains do not ensure required accuracy of strength assessment and are of practically no use in design of optimal structures with low construction costs and material consumption. Therefore, failure criteria ensure not only reliability of calculations, but also, eventually, development of optimal structures intended to operate at low temperatures. To this effect, it would be practicable to analyse drawbacks in current definitions of failure criteria, to develop more efficient ones and compare the efficiency of the old and the new criteria taking into account failure test data on the samples with stress concentrators.

2. BRITTLE FAILURE CRITERION

Brittle failure of metal structures of ships and other marine facilities is generally unacceptable. Kopelman (2010) shows that brittle failure of structural material occurs when certain grains of polycrystal material have defects in their structure, i.e. sub-microcracks, so that:

$$\sigma_1 \geq S_{rupt}, \quad (1),$$

where σ_i is intensity or equivalent Mises stress; σ_1 - maximum principal stress; S_{rupt} - normal rupture stress independent on the temperature of tests.

Makhutov (1981) suggests the assessment formula for normal rupture stress:

$$S_{rupt} / \sigma_{\sigma} = 1 + 1.4\psi_{\kappa},$$

where ψ_{κ} is relative necking of standard sample at rupture; σ_{σ} - ultimate strength.

Kopelman (2010) shows that minimum rupture stresses S_{rupt} of structural steels depend on

their ferrite grain sizes d_g :

$$S_{rupt.} = 20 + 11.5\sqrt{d_g}, \text{ kg/mm}^2 \text{ (} d_g \text{ unit is mm).}$$

This formula shows that, in order to ensure high $\sigma_{rupt.}$ and σ_g values of perlite steels, metallurgists and technologists should, at all stages of metal production and processing, take measures for making these grains as small as possible. Along with it, this formula somewhat contradicts one of the basic postulates of deformable solid mechanics. Indeed, it implies that, on the one hand, strength of material depends on its grain size, i.e. on its non-uniformity at the micro-level. On the other hand, according to the continuity hypothesis of deformable solid mechanics, grained structure of material can be ignored in calculations. Besides, damage accumulation in material prior to its brittle fracture is accompanied by initiation of sub-microcracks and voids, so, strictly speaking, strain continuity equations cannot be true in this case.

The way out of this situation is suggested in Neuber-Novozhilov theory that assumes that conditions for initiation and development of sub-microcracks finally resulting in material failure, form at some finite volume of material, rather than at some specific point. This volume would be useful to associate with the notion of structural element with size d , dependent on material parameters (micro-level non-uniformity) in specific failure scenarios. This size d is determined as per the formula given in Morozov et al. (2011),

$$d = 2K_{Ic}^2 / (\pi S_{rupt.}^2), \quad (2),$$

where K_{Ic} is fracture toughness.

For carbon and low-alloyed steels, d is generally 3-7 mm.

Common Neuber-Novozhilov integral criterion of brittle strength compares true rupture stresses $S_{rupt.}$ not versus maximum positive values of the first principal stress σ_1 (as seen from Formula(1)), but versus the mean normal stress, i.e.

$$\bar{\sigma}_n = \iint_F \sigma_n dF / F$$

at site F with the area of about d^2 , including an infinitely small site with normal line \vec{n} , where maximum principal stress σ_1 acts in the stress concentrator under investigation. In this formula, σ_n is normal stress at site F . In the particular case of stress concentration near a circular opening in a wide strap with thickness t (Fig. 1) under tension, area F is equal to product td .

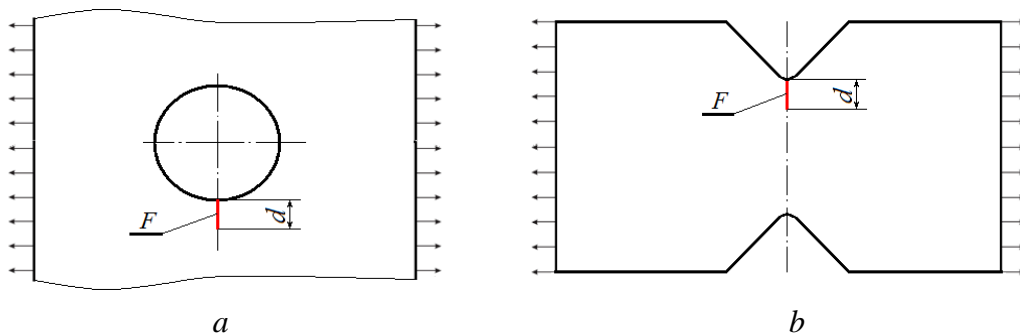


Fig. 1. Strap samples under tension. Site F of structural element with size d (see (2)), with infinitely small site where maximum principal stress σ_1 acts in stress concentrators near circular opening (a) and V-notch (b)

Thus, instead of maximum stress criterion (2), brittle failure inception can be determined as per Neuber-Novozhilov approach and the following integral criterion:

$$\bar{\sigma}_n \geq S_{rupt}, \quad (3),$$

where $\bar{\sigma}_n$ is normal stress in the concentration zone averaged by site F .

Instead of local yield criterion (1), it is possible to use the integral criterion

$$\bar{\sigma}_i \geq \sigma_m, \quad (4),$$

where $\bar{\sigma}_i = \iint_F \sigma_i dF / F$ is mean stress intensity at site F .

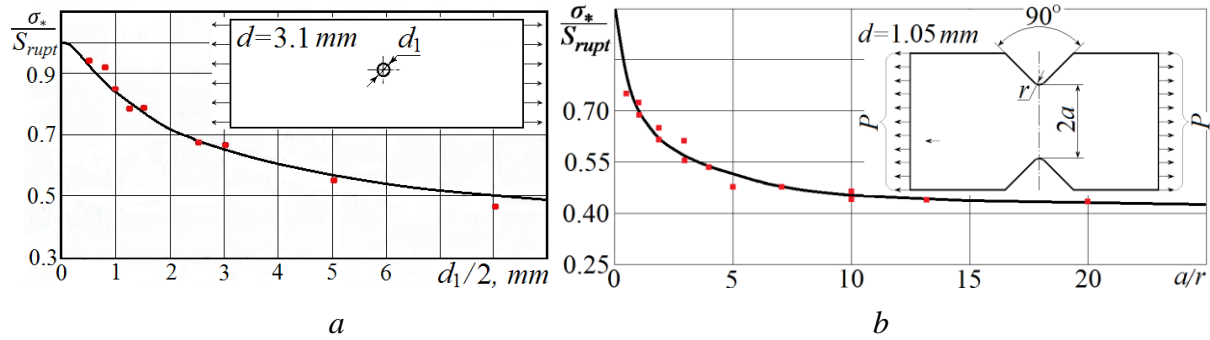


Fig. 2. Calculated (solid curves) and experimental (red dots) nominal failure stresses σ_* as fractions of rupture stresses S_{rupt} , versus design parameters of samples: a – strap with circular opening; b – strap with V-notches (Fig. 1 illustrates size d of structural element)

Greater efficiency of integral brittle failure criteria (3) and (4), as compared to maximum-stress criteria (1) and (2) can be illustrated by the test data for thin straps with stress concentrators (circular perforations of various radii), made of brittle material (gray iron SCh 24-48 with $d = 1.4$ mm, see Morozov, et al. (2011)). The width of these straps was much greater than the perforation diameter. Fig. 2a compares these test data against calculation results for nominal failure stresses σ_* (as fractions of rupture stress S_{rupt}) versus concentrator radius. Analytical and experimental data suggest that the theoretical coefficient of stress concentration and criteria (1) and (2) can give ultimate stresses only for wide straps with large openings (radius 10+ times greater than d). In this case, calculated failure stresses are three times lower than those observed in the experiment. At low radii of openings, the results obtained as per local brittle strength criteria (1) and (2) are even lower, which makes accurate strength predictions impossible.

Fig. 2b illustrates test data for grey-iron strap with V-notches (Morozov, et al., 2011). Ultimate strength of iron is 270 MPa, $d = 1.05$ mm. Neck width was the same in all the experiments, $2a = 16$ mm. Curvature radius r at the notch tip varied between 0.4 and 16 mm. Comparison of the test data versus calculation results obtained as per integral criteria (3) and (4) confirms that these criteria yield credible results in the whole range of curvature radii at notch tip. Credibility of the analytical curve is also confirmed by the fact that it asymptotically tends to theoretical value $\sigma_*/S_{rupt} = 0.4$, which corresponds to $a/r \rightarrow \infty$, i.e. to edge fracture.

Other test data also lead to similar conclusions, i.e. that integral brittle failure criteria (3) and (4) are credible and practicable to use instead of local criteria (1) and (2). M. Legan and V. Blinov (2015) performed tension tests on the straps with the same thickness made of other brittle material (ebonite) with circular openings of various diameters, see Fig. 3. The ratio between opening diameters and strap thicknesses during these tests was not always the same.

Test results are given in Table 1.

Table1. Dimensions and failure stresses of strap specimens (actual (σ_*) and calculated)

Diameter d , mm	Test section length, mm	Test section width, mm	Specimen thickness, mm	Experimental rupture stress σ_* , MPa	Rupture stress calculated as per Criteria (3) and (4), MPa	Rupture stress calculated as per Criteria (1) and (2), MPa
5	135	49.86	8.24	33.7	24.7	13.0
2	65	9.83	8.03	35.0	29.8	12.5
1	65	9.56	8.00	38.1	33.9	13.1

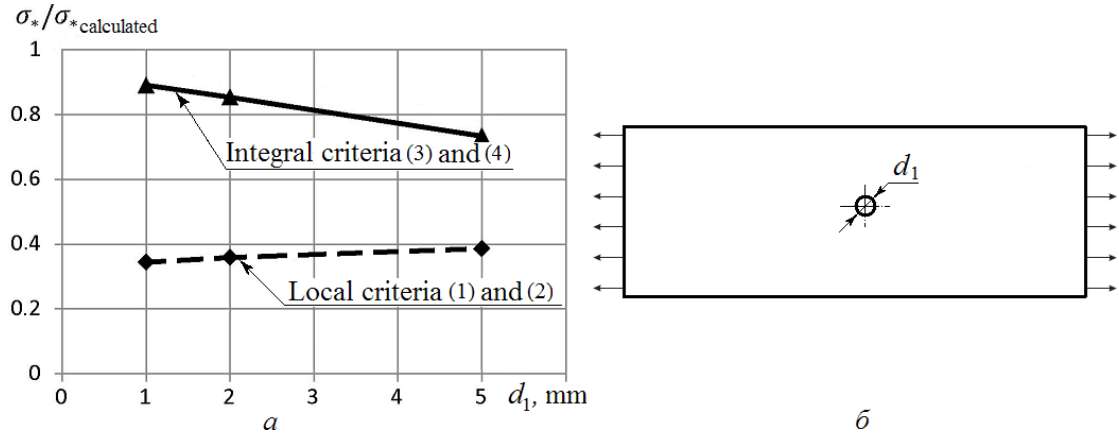


Fig.3. *a* – ratio between experimental (σ_*) and analytical ($\sigma_{*calculated}$) nominal failure stresses of perforated strap specimens versus perforation diameter d_1 ; *b* – illustration of tension test setup

Ideally, $\sigma_*/\sigma_{*calculated}$ should be 1. However, in reality, failure stresses calculated as per integral criteria (3) and (4) are considerably, although not very much, different from the corresponding test results. If perforations are small, failure stress calculation as per maximum-stress criteria (1) and (2) yields the results more than 2 times different from the test data.

Compression failure tests of perforated ebonite disks described in Legan (2013), see Fig. 4 below, also give an opportunity to evaluate efficiency of integral brittle strength criteria. The results of these tests also suggest that calculation results obtained as per integral criteria (3) and (4) have much better correlation with the test data. Again, if perforations are small, limit loads obtained as per local brittle strength criteria (1) and (2) are several times lower than in reality.

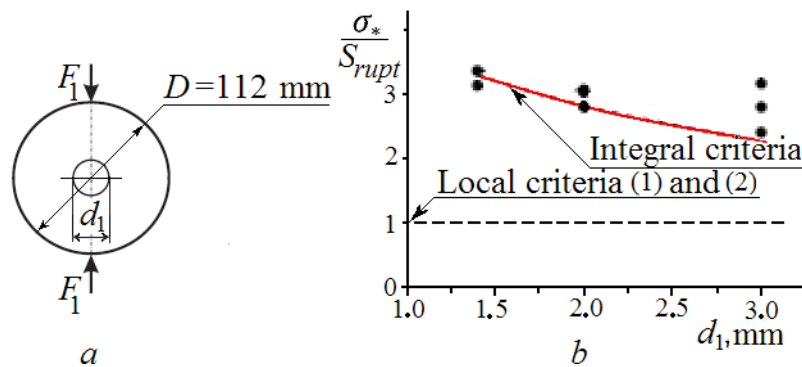


Fig 4. *a* – setup of compression failure tests on ebonite disk; *b* – comparison of experimental failure stresses (dots) versus calculation results obtained as per the integral criterion (red curve) and the criterion of maximum principal stress (black dashed line)

Comparison of calculation results and test data leads to the following conclusions:

- For stress concentrations with rather high non-uniformity of distribution, analytical estimates of failure loads based on local brittle failure criteria (1) and (2) are too low;
- Integral criteria (3) and (4) yield the estimates sufficiently close to real values;
- If stress concentrations have small characteristic size, i.e. if the radii of perforations or notch tip roundings are small as compared to structural element size d , local brittle strength criteria (1) and (2) give too low failure loads;
- As operational temperatures go down to the levels corresponding to ductile-brittle transition, failure pattern of materials and welded joints becomes less ductile, which results in smaller d and lower failure loads in sharp notches and concentrators.

As a rule, stress concentration factor of structural joints is between 1.5 and 3.5, and rupture resistance is 2-3 times above the yield strength of steel. If this factor is higher ($\sim 2.8-3.5$), there is a great probability of brittle failure (cracks in concentrators) at nominal structural stresses below yield strength of its material and at the temperatures considerably above the ductile-brittle transition point.

3. DUCTILE FAILURE CRITERION

Ductile failure criterion is commonly taken as ratio between achieved plastic strain intensity e_{pi} and limit intensity e_p^{lim} (critical level of straining when voids merge, forming ductile cracks). This straining criterion, see Makhutov (1981) for more details, is based on the physical model of plastic loosening and, in its simplest form, can be expressed as inequality true for peak plastic straining point e_{pi} :

$$e_{pi} \geq e_p^{\text{nped}}. \quad (5)$$

Plastic straining intensity e_{pi} can be defined as function of principal plastic strains e_{p1} , e_{p2} and e_{p3} for the point (or element) under investigation:

$$e_{pi} = \frac{\sqrt{2}}{3} \sqrt{(e_{p1} - e_{p2})^2 + (e_{p2} - e_{p3})^2 + (e_{p3} - e_{p1})^2}.$$

The most important factor of plastic straining of material is stress intensity:

$$\sigma_i = \frac{\sqrt{(\sigma_1 - \sigma_2)^2 + (\sigma_2 - \sigma_3)^2 + (\sigma_3 - \sigma_1)^2}}{\sqrt{2}},$$

Where $\sigma (1, 2, 3, \dots)$ is principal stress.

Average stress $\sigma_0 = (\sigma_1 + \sigma_2 + \sigma_3)/3$ does not result in any plastic straining and only leads to elastic variations of volume. At $\sigma_i = 0$ any metal is elastic and brittle. If maximum principal stress $\sigma_1 < 0$, i.e. if compression load is applied, micro- and macrocracks close, making metal more plastic. If metal is exposed to three-axial tension, which is often the case for sharp stress concentrators in structures, its plasticity drops sharply. Taking this into account, intensity of plastic failure strain e_k in stress concentration zone is calculated with consideration of σ_i / σ_0 ratio, see Makhutov (1981):

$$e_k = D_e e_p^{\text{lim}}, \quad (6)$$

where $D_e = K_e \sigma_i / (3\sigma_0)$ is plastic strain reduction coefficient, and e_{p1}^{lim} is limit plastic strain,

determined as per uniaxial tension test data for standard cylindrical specimens; K_e - coefficient taking into account the properties of given material (for low-carbon steel, $K_e = 1.0 - 1.2$).

Formula (5) is confirmed by the tests of big specimens made of various steels and having rather large stress concentrators of various shapes, see Makhutov (1981).

Failure criterion (5) means a rupture (crack) in the stress concentration zone of a real welded structure. However, this criterion does not give any hints on possible patterns of crack development. Depending on material, geometry and loading conditions of given structure, crack may stop immediately after its initiation, or else it may develop further, breaking the structure into pieces. However, even very small cracks dramatically reduce fatigue life and reliability of structure, as well as increase probability of leaks. In most of cases, this state of structure is not normal. Ductile failure criterion (5) can be also expressed as:

$$e_{pi} / (D_e e_p^{\text{lim.}}) \geq 1. \quad (5')$$

Criterion (5') is true for peak plastic straining pointing given stress concentrator, so it is a local criterion. However, as it has already been noted above for the brittle failure pattern, integral criteria yield more accurate predictions than local ones. This seems to be true for the ductile failure pattern, too, because final stages of both brittle and ductile failure are somewhat similar. Indeed, ductile failure begins once plasticity limit of the material is achieved, and ends up with initiation and development of micro-defects in the structure of material (voids and sub-microcracks). Merging and developing, these micro-defects evolve into macro-cracks, and these, developing rapidly, finish the failure process. However, this process is typical for brittle failure, too, and takes place not at some specific point, but within some area where straining is the greatest. In other words, the site of macro-crack initiation is not infinitely small, but has some finite size, and Formula (6) holds true for its greater part. It means that parameters e_{pi} and D_e in this formula, as well as other parameters of stress-strain state (the fraction in the left part of Expression (7) below) describing the failure process, have to be averaged for a certain area. Due to this similarity in final stages of both ductile and brittle failure, this site can be regarded as above-mentioned area F with linear size d . Taking this into account, strain-based integral failure criterion can be expressed as:

$$\bar{e}_{p1} \geq 1, \quad (7),$$

where $\bar{e}_{p1} = \frac{1}{e_{p1}^{n_{ped.}} F} \int_F \frac{e_{pi}(x, y, z)}{D_e(x, y, z)} dF$ characterizes ductile damage of material with infinite

site F , containing the point with the highest e_{pi}/D_e ratio in given stress concentrator, and an infinitely small principal site within this point where principal stress σ_1 is applied.

This parameter is equal to the average corrected (i.e. conditionally reduced to uniaxial stressed state) intensity of plastic straining at site F with the area of $\sim d^2$, perpendicular to principal stress σ_1 and containing the point with the highest e_{pi}/D_e (this ratio characterizes generation intensity of voids and other micro-defects at specific point of material for the given type of stressed state).

Kryzhevich (2017) gives recommendations on practical assessment of D_e coefficient and demonstrates that these recommendations yield reliable results fairly close to actual values.

4. ANALYTICAL AND EXPERIMENTAL VALIDATION OF DUCTILE FAILURE CRITERION

To obtain experimental data and compare them versus calculation results, the tests were performed on 12 smooth cylindrical samples made of experimental steel for Arctic applications (provisional name 750W). The samples were manufactured as per GOST 1497-84. Besides, the tests were performed on 8 additional cylindrical samples made of the same steel, but having a stress concentrator (circular V-notch, depth 1 mm, opening angle 60°, made as per GOST 25.502-79, see Fig.5 below). The samples were cut from rolled plates (thicknesses 25 mm and 40 mm, 10 samples for each thickness (6 smooth, 4 notched)). A half of all the samples (both smooth and notched) was subjected to tension failure tests at room temperature (20°C), another half was subjected to similar tests at temperature -40°C, see Table 2.

During the tests on smooth samples, mechanical parameters of 750W steel were determined as per GOST 1497-84.

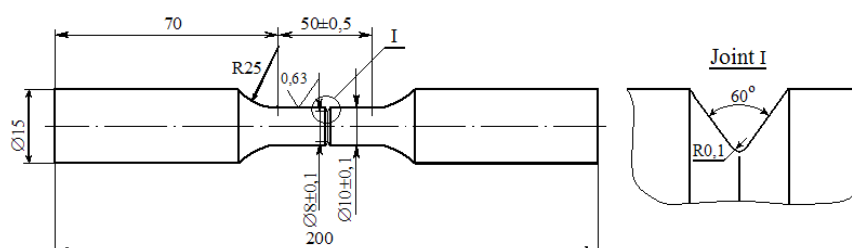


Fig. 5. Sketch of notched samples used in tension tests

Table 2. Effect of temperature, stress concentration and plate thickness upon strength of 750W steel samples

No.	Type of sample and temperature of tests	Min. dia, mm	Ultimate strength, MPa	Yield strength, MPa	Plate thickness	Failure elongation, mm	Max load, kN
1	Smooth +20°C	9.9	856	816	25 mm	6.82	65.93
2		9.88	854	801		7.02	65.5
3		9.8	859	817		6.01	64.83
4	Smooth -40°C	9.9	879	845		7.13	67.71
5		9.9	885	849		7.06	68.09
6		9.9	885	851		6.9	68.15
7	Notched +20°C	8	-	-		1.29	60.02
8		8	-	-		1.32	60.06
9	Notched -40°C	8	-	-		1.26	60.43
10		8	-	-		0.99	60.15
11	Smooth +20°C	9.8	869	823	40 mm	3.02	65.58
12		9.82	851	811		5.41	64.48
13		9.9	877	835		5.42	67.55
14	Smooth -40°C	9.8	898	858		6.95	67.72
15		9.9	885	849		7.15	68.10
16		9.8	894	854		7.33	67.41
17	Notched +20°C	8	-	-		1.27	61.11
18		8	-	-		1.68	61.00
19	Notched -40°C	8	-	-		0.45	61.08
20		8	-	-		0.33	60.94

The tests were performed by KSRC at LFV-250-HH servo hydraulic universal test machine, see Fig.6, in accordance with GOST1497-84 (Metals, Tension Tests, Methods) and GOST 11150-84 (Metals, Tension Tests at Low Temperatures, Methods). Relative error in test load was $\pm 0.5\%$, confidence level 95%. The machine had a special climatic chamber for generation of low temperature.

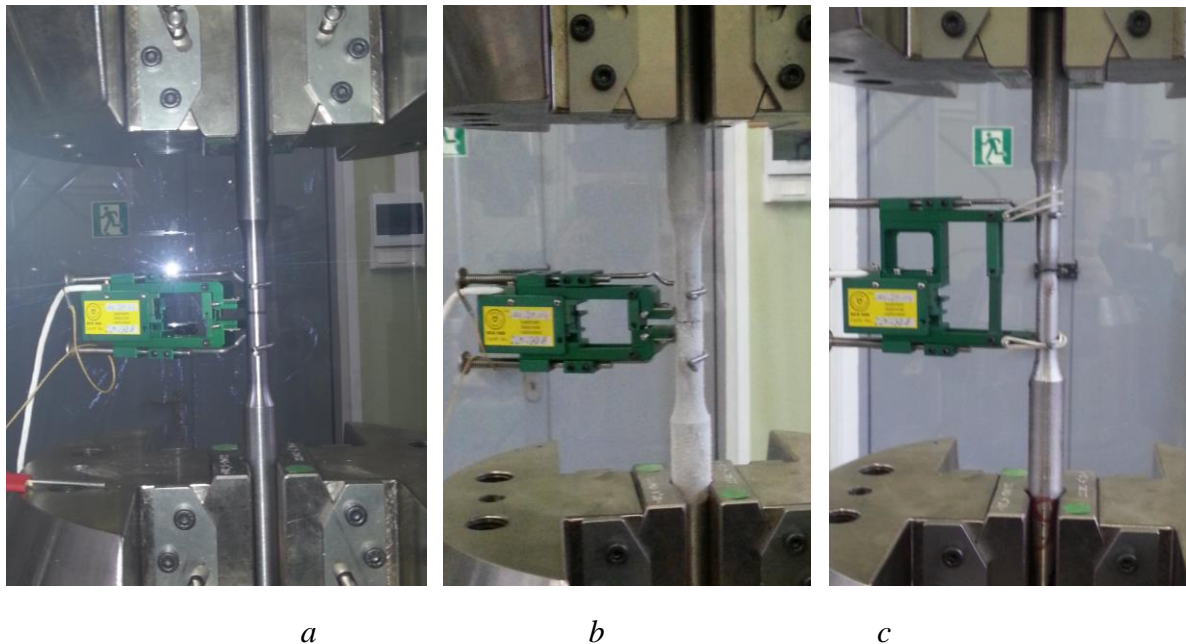


Fig.6– Tests of notched samples: *a*) room temperature; *b*) low temperature; *c*) broken sample in test machine clamps after failure test.

Test data (see Table 2 above) show that temperature decrease by 60°C improved ultimate strength by $\sim 3\%$ and yield strength by $\sim 4\%$. Greater thickness of samples slightly (by $\sim 1\%$) improved their yield and ultimate strength. Meanwhile, for the smooth samples, 60°C temperature decrease led to a minor growth of their failure load levels, as well as to slightly greater residual strains at the moment of their failure. For the notched samples, things were quite different: temperature decrease had little or no effect upon failure loads, and residual strains decreased considerably: at the average, by 14% for thinner samples and by 74% for thicker ones. The reason for this is that ductile-brittle transition point of the tested material, as determined in accordance with ASTM E 208-06 (2012) standard, was below the temperature of tests (-40°C).

It is especially important to note that decrease in residual strains of the samples at low temperature is mainly due to two factors: plate thickness and stress concentration. At fixed thickness, average decrease in residual strains of samples due to stress concentrator was 6.25 times for 25-mm thick samples and 18 times for 40-mm thick ones. At fixed stress concentration, increase in thickness results in 2.9 times (at the average) lower residual strains. The figures given in Table2 also suggest interaction of these two factors.

Shape and parameters of tension diagrams for the samples considerably depend on the type of sample (smooth/notched) and temperature of tests, see Fig. 7 below. Notched samples have lower residual strain after failure (especially at low temperature) and also show some signs of dynamic plastic straining (vibration due to development of plastic straining zones). Average normal stresses in structural grains of the samples at the moment of failure mostly differed from rupture stresses by not more than 12%.

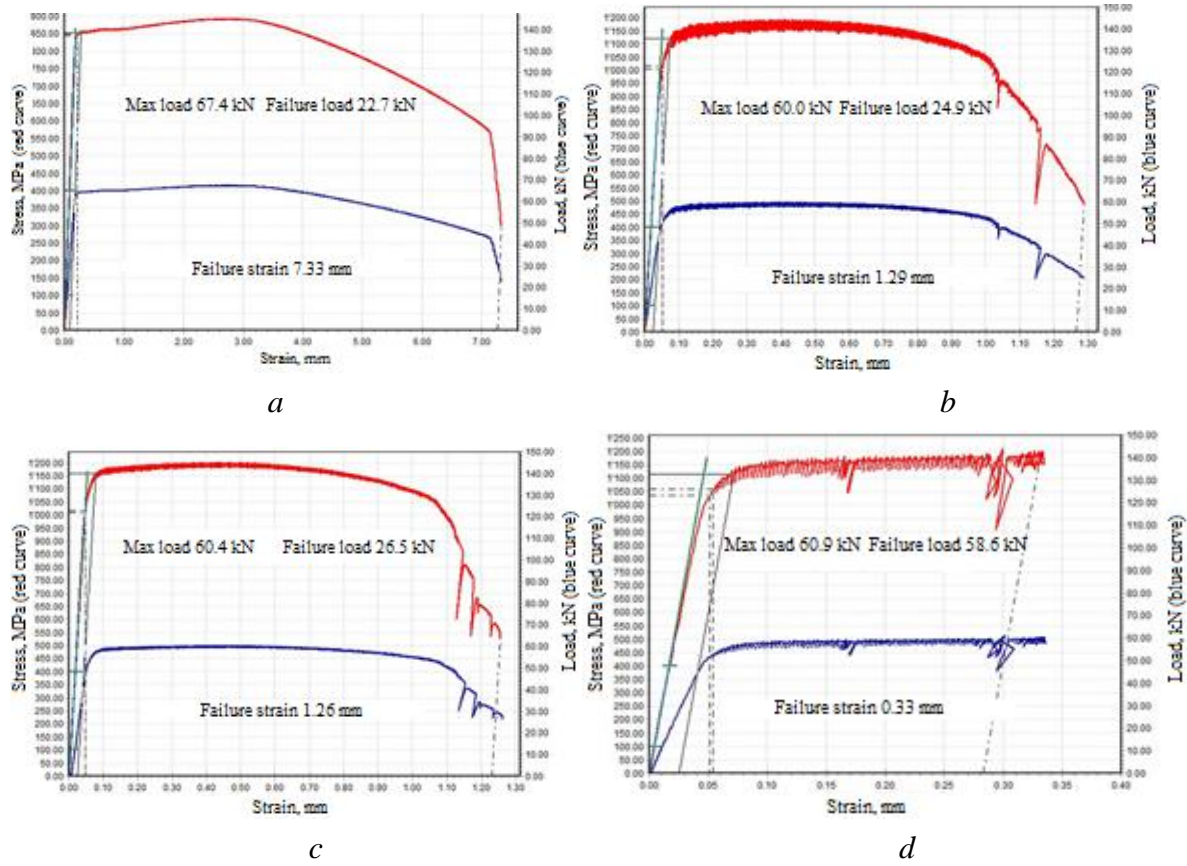


Fig. 7– Loads (blue curves) and stresses (red curves) in smooth part of samples versus total straining: *a* – smooth sample, thickness 40 mm, temperature -40°C ; *b* – notched sample, thickness 25 mm, temperature $+20^{\circ}\text{C}$; *c* – notched sample, thickness 25 mm, temperature -40°C ; *d* – notched sample, thickness 40 mm, temperature -40°C .

Maximum loads recorded on the same samples at room and low temperature were quite close, which might mean that plastic straining of samples is accompanied by inception of pre-failure nuclei (structural elements) in stress concentration zones, and these nuclei might have approximately the same size, well above the size of stress concentrator (~ 1 mm). This is confirmed by finite-element calculations in ANSYS software package. Finite-element model of the notched sample represented $1/8^{\text{th}}$ part of it, see Fig. 8 below. The sample was symmetric with respect to the plane perpendicular to its axis and passing via the tip of the notch, so the displacements along the axis of the sample in this plane are assumed as zero ($U_x = 0$). In mutually perpendicular planes passing via the axis of the sample, normal displacements are also assumed as zero ($U_y = 0$ and $U_z = 0$). In the plane located 25 mm away from the tip of the notch and perpendicular to the axis of the sample, displacements along this axis are assumed as the same and not equal to zero ($U_x \neq 0$).

Calculations have shown that growth of plastic straining at the tip of the notch (up to the limit values corresponding to crack initiation) occurs when the stresses far from the notch do not exceed yield strength of the sample. The tip of the notch has stress-strain state with stiffness coefficient at the moment of failure equal to ~ 1.4 . Although the notch is not very deep (1 mm), as compared to the structural parameter $d = 3.2$ mm, it still brings about considerable (down to 13%) reduction of the specimen's limit load.

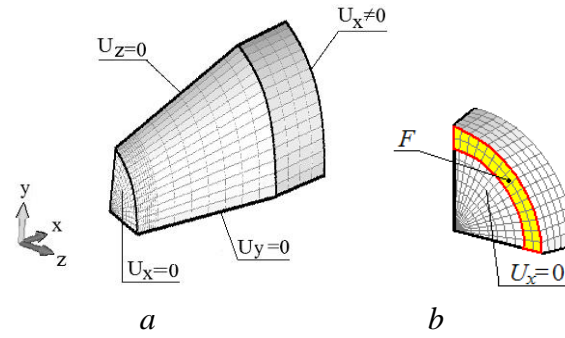


Fig. 8. Finite-element model of notched specimen (a) and its fragment (b):

Yellow colour highlights structural element in the plane perpendicular to the specimen axis and passing via the notch tip

Stress-strain state at the concentrator is three-dimensional, which restricts plastic straining to rather great extent. Therefore, a sharp stress concentrator like this might make the structure fail even at global (nominal) stresses below its yield point. Fig. 9 below compares experimental failure stresses and calculated nominal stresses of the specimen obtained as per local ductile strength criterion (5) and integral criterion (7). This figure clearly shows that integral criterion gives considerably more accurate predictions of limit loads. Thus, formulating a ductile failure criterion, limit-equilibrium state of a structure is preferable to describe by means of the integral relationship between stress-strain state of its joints (averaged within structural element) and parameters of its materials. Here, the parameters characterizing pre-failure behavior specifics of materials, i.e. dimensions of structural elements, should be taken into account, especially if they are almost the same as characteristic dimensions of stress concentrators.

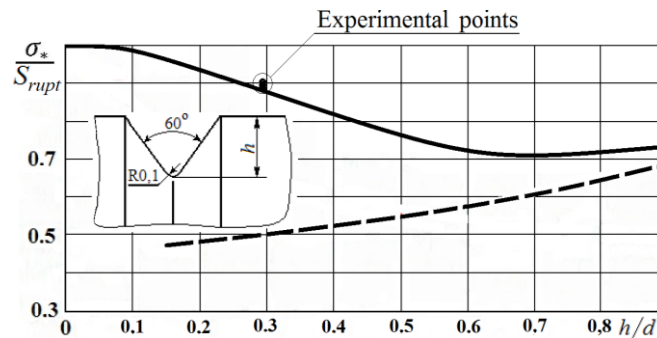


Fig.9. Rupture stresses σ_* of notched samples: solid curve - finite-element calculation results as per integral criterion (7); dashed curve – corresponding calculation results as per local criterion (5); dots – experimental points

Thus, to calculate ultimate low-temperature strength of a structure is to check if brittle criterion (3) holds true. If this is not the case, structural failure will be accompanied by residual strains in the stress concentration zone, so it will be necessary to apply strain-based failure criterion (7). Anyway, criteria (3) and (7) enable calculation of the minimum failure load for some weak joint of a structure. These calculation results for failure (limit) loads Q_p can be compared versus maximum operational loads Q_{\max} . Then, static strength condition can be written as:

$$Q_p/Q_{\max} \geq k_m,$$

where k_m is ultimate strength margin.

MAIN CONCLUSIONS

The main results of the experiments and calculations described above are as follows:

- Analysis of drawbacks in conventional approaches to low-temperature strength calculations for marine structures;
- Development of mathematical models for brittle and ductile failure of structures at low temperature, as well as development of corresponding integral criteria of ultimate strength based on the idea of initiation of pre-failure zones (structural elements) in the vicinity of stress concentrators that tend to diminish as temperature goes down.
- Development of FEA-based calculation method for limit loads leading to brittle or ductile structural failures of marine facilities at common and low temperatures.
- Failure tests of notched samples made of steel for Arctic applications have yielded the data on low-temperature failure specifics within stress concentration zones. Comparison of calculation data versus test results has shown that integral criteria of low-temperature strength suggested in this paper give considerable more accurate predictions of failure loads for Arctic structures;

REFERENCES

1. American Bureau of Shipping Rules for Building and Classing - Steel Vessels, 2016.
2. ASTM E 208-06 (2012) Standard Test Method for Conducting Drop-Weight Test to Determine Nil-Ductility Transition Temperature of Ferritic Steels, ASTM International, 2012.
3. Bureau Veritas Rules for the Classification of POLAR CLASS and ICEBREAKER Ships, 2013.
4. Draft ISO/DTS 35105.2:2017(E). Petroleum and Natural Gas Industries — Arctic Operations — Material Requirements for Arctic Operations. DTS stage, 2017
5. GOST R ISO19906 Standard. Petroleum and Natural Gas Industries – Arctic offshore structures (*Russian translation*). Moscow, Standartinform, 2011.
6. Hauge M. Arctic Offshore Materials and Platform Winterization. Proceedings of the Twenty-second (2012) International Offshore and Polar Engineering Conference, Rhodes, Greece, June 17-22, 2012.
7. Horn A.M., Hauge M. Material Challenges for Arctic Offshore Applications, a Reliability Study of Fracture of a Welded Steel Plate Based on Material Toughness Data at -60°C. Proceedings of the Twenty-first (2011) International Offshore and Polar Engineering Conference, Maui, Hawaii, USA, June 19-24, 2011.
8. ISO 19902:2007 Standard. Petroleum and Natural Gas Industries – Fixed Steel Offshore Structures (*Russian translation*), 2016.
9. *Kopelman L.* Fundamentals of Strength Theory for Welded Structures. St. Petersburg, Lan', 2010 (*in Russian*).
10. *Kryzhevich G.*, Fatigue Strength of Steel Structures at Low Temperatures // *Morskoy Vestnik*, 2017. Special Issue No. 1 (13), pp. 66-70 (*in Russian*).
11. *Kryzhevich G.*, Strength of Thick-plated Welded Structures of Ships and Marine Facilities in the Arctic. // *Transactions of KSRC*, 2017, Issue 380, pp. 32-41 (*in Russian*).
12. *Legan M., Blinov V.*, Joint Application of Boundary-element Method and Non-local Failure Criteria // *Omsk Scientific Bulletin*. 2015, No. 3 (143), pp. 349-352 (*in Russian*).
13. *Legan M.*, Brittle Failure of Structural Elements with Stress Concentrators // *Vestnik NSU*. 2013. Vol. 13, Issue 3, pp. 70-76 (*in Russian*).
14. *Makhutov N.*, Straining Criteria and Strength Calculations of Structural Elements. Moscow, Mashinostroyeniye, 1981 (*in Russian*).

15. *Morozov N., et al.* Limit Equilibrium of Brittle Bodies with Stress Concentrators. Structural Approach. St. Petersburg, Publishing House of St. Petersburg State University, 2011 (*in Russian*).
16. *Neuber H.*, Kerbspannungslehre: Grundlagenfür Genaue Spannungsrechnung (*Russian translation*). Moscow-Leningrad, Gostekhizdat, 1947, 204 pp.
17. Rules for Classification and Construction of Sea-Going Ships. St. Petersburg, Russian Maritime Registry of Shipping, 2016.
18. Rules for the Classification, Construction and Equipment of Mobile Offshore Drilling Units and Fixed Offshore Platforms. St, Petersburg, Russian Maritime Registry of Shipping, 2014.
19. Wallin K., Karjalainen-Roikonen P., Low-Temperature Fracture Toughness Estimates for Very High Strength Steels. International Journal of Offshore and Polar Engineering (Transactions of The International Society of Offshore and Polar Engineers). Vol. 26, No. 4, December 2016, pp. 333-338.